Discussion

Although the original field relations of the peridotites described in Sections 5.3.1 and 5.3.2 are not preserved, it is quite conceivable that they are fragments of minor intrusives analogous, at least in mode of occurrence, to the vein-like, dyke-like or pod-like dunitic and/or pyroxenitic intrusives in the tectonized harzburgites of some ophiolites e.g. Othris and Troodos (Menzies and Allen, 1974), Vourinos (Harkins *et al.*, 1980), Bay of Islands (Malpas, 1978), Canyon Mountain (Himmelberg and Loney, 1980), Dun Mountain (Challis, 1965) and Oman (Boudier and Coleman, 1981). Few data are available on rocks of this type in other ophiolitic assemblages. It must be emphasized, however, that the PBOC rocks under discussion are mineralogically and chemically quite dissimilar to the comparatively *di*-rich gabbros and wehrlites, interpreted as partial melt segregations sometimes found in the tectonized harzburgites of the above-cited ophiolites. Nevertheless, it is possible that the PBOC olivine orthopyroxenites might be early-formed cumulates crystallized from *en*-rich melts which were derived from a relatively depleted upper mantle; that is, melts of the type which may have been parental to the PBOC olivine norites (see Section 5.4). If the relatively Fe-rich plagioclase-bearing peridotites are derivatives from such liquids, then their relatively high Ni, Cr and/or OL abundances (Fig. 5.9, Table 5.1) suggest that crystallization may have taken place under more-or-less open system conditions (*cf.* Church and Riccio, 1977; O'Hara, 1977).

5.3.3 Sedimentary Serpentinite

At GR 7125,9143, fossiliferous clastic rocks consisting almost entirely of serpentinite fragments and serpentine minerals form a small rubbly lensoidal outcrop (~40 m x 10 m) within, but at the very margin of the Watchimbark Serpentinite. Along its western margin this lens of sedimentary serpentinite is in tectonic contact with highly schistose, 'normal' serpentinite. Where exposed, this contact (I exposed this contact by digging and blasting) is sub-vertical, and steeply-plunging slickensides are abundant on the surfaces of both serpentinite types. Within the sedimentary serpentinite itself, variably-oriented slickensides are abundant on what would otherwise appear to be joint surfaces. This suggests that the outcrop is disrupted by numerous small faults and is

at least incipiently brecciated. In fact, the very close spatial association between coarse and fine clastics (see below) in this outcrop might reflect some tectonic mixing of proximal and distal serpentinite sediments during their incorporation into the schistose serpentinites. Nevertheless, some coarse-grained horizons do grade abruptly into fine-grained horizons over centimetre-scale intervals (sample 271). The eastern margin of the sedimentary serpentinite is not exposed but it is most probably faulted against polymictic pebbly sandstones and coarse siltstones of the Manning Group which crop out several tens of metres to the east. I could not detect serpentine minerals in these Manning Group rocks (samples 266, 267, 277-279) by petrographic and XRD examination, nor is Cr-Al spinel or serpentine present in their magnetic fractions. However, Benson (1913) found a pebble of serpentinite in Manning Group sandstones (*cf.* Voisey, 1939) in the "Newcastle district" to the (?) southeast of the Pigna Barney - Curricabark area. Prior to this study, the Benson pebble was the only evidence to suggest that at least some serpentinized peridotites in the NEO were exposed to erosion in the Permian. Although serpentinized peridotites are relatively widespread in eastern Australia, derivative clastic rocks are comparatively rare (see Crook and Felton, 1975 for a summary).

The PBOC sedimentary serpentinite is well-lithified and consists of poorly-sorted, diffusely stratified, coarse-grained pebbly sandstones (Plate 5.3A,B) and pebble-free (generally), comparatively well-sorted medium-to fine-grained sandstones. The latter may display cross-stratification and graded bedding (samples 271, 272) but, although they are relatively well-stratified, individual sedimentation units are generally rather poorly defined. Although the outcrop is too disrupted to allow detailed sedimentological analysis, mesoscopic fabrics noted above suggest that sedimentation occurred *via* a combination of mass-flow and turbidity current mechanisms.

Petrography

Pebbles in the coarse-grained sandstones seldom exceed 3 cm in size and are almost entirely fragments of completely serpentinized peridotite (e.g. 261, 165). These are accompanied by extremely rare pebbles of microlitic mafic volcanics (e.g. 273) and lithofeldspathic

PLATE 5.3

PBOC Sedimentary Serpentinite:

A. Medium- to coarse-grained, poorly sorted pebbly serpentinite sandstone. Valve of juvenile *Eurydesma* lies in the plane of diffuse bedding. Pale intergranular patches on the highly oblique face and in the upper left part of the slightly oblique face are structureless serpentine cement. Marginal scale graduated in millimetres [sample 280].

B. Unidentified articulated bivalve mollusc embedded in poorly-sorted coarse-grained serpentinite sandstone. Note pale intergranular serpentine cement. Marginal scale graduated in millimetres. [sample 281].

C. Rounded pebble of altered 'lithofeldspathic' sandstone of (?) mafic volcanogenic provenance accompanied by a small angular mafic volcanic fragment in medium-grained serpentinite sandstone. Pale grains in the sandstone pebble consist of chlorite ± serpentine presumably pseudomorphing plagioclase. Note disseminated intergranular Cr-Al spinel (black subhedra) and magnetite (black anhedra), and secondary magnetite within clasts. The remaining grains are serpentinite. The 'mottled' area in the upper left corner of the photograph reflects partial disaggregation of that part of the thin section during grinding. [sample 268, mag. = 6x , transmitted tungsten light].

D. Subangular microlitic quench-textured mafic volcanic fragment in serpentinite sandstone. Plagioclase microlites are pseudomorphed by chlorite ± serpentine. Black grains in the matrix are predominantly Cr-Al spinel with occasional irregular magnetite overgrowths. The remaining fragments are serpentinite [sample 260, mag. = 22x , plane-polarized light].

E. Rounded clast consisting almost entirely of (?) bladed antigorite in medium-grained serpentinite sandstone [sample 274, mag. = 35x , crossed nicols].

F. Bladed antigorite (?) in Watchimbark serpentinite *cf.* Plate 5.3E. [sample 435, mag.= 35x , crossed nicols].

G. Cumulus texture in serpentinized harzburgite clast. Pale grains with postcumulus overgrowths and partially intergranular habits are bastite after orthopyroxene. Dark areas consist of serpentinized olivine [sample 260, mag. = 22x , crossed nicols].

H. Tectonized harzburgite pebble in serpentinite. Note spinel-'orthopyroxene' (bastite = 0) habits similar to those in some PBOC tectonized harzburgites, *cf.* Plate 5.1) [sample 264, mag. = 9x , plane-polarized light].

PLATE 5·3

A

B

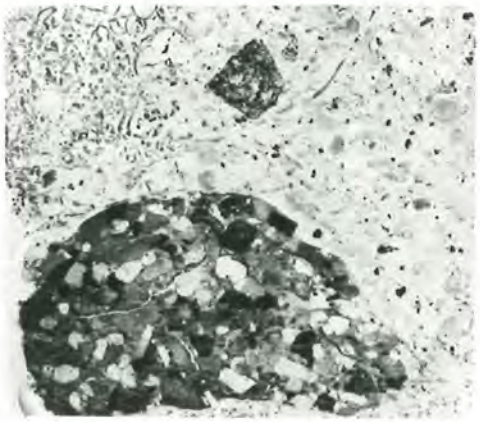

C

D

E

F

G

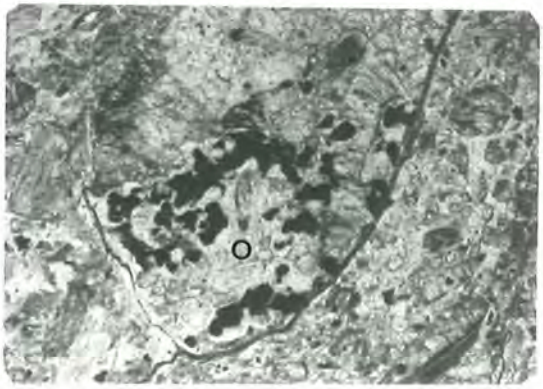

H

sandstone of mafic volcanic provenance (Plate 5.3C). The matrix predominantly consists of angular-to sub-rounded serpentinite fragments, bastite and (?) serpentinized olivine fragments, up to several percent of microlitic mafic volcanic fragments (Plate 5.3D) and disseminated detrital magnetite and Cr-Al spinel. Some samples (e.g. 274) contain up to *ca* 15% of essentially structureless tan (in thin section) or cream (in hand specimen) cement (Plate 5.3A) which approximates to serpentine in chemical composition.*

Relative to the rocks described above, the medium- and fine-grained serpentinite sandstones contain a higher proportion of discrete serpentinized ferromagnesian crystal fragments, possibly as high as 70% in sample 265 (such fragments are often difficult to identify with complete confidence). No relict grains of olivine or pyroxene were observed in any of the 41 thin sections of sedimentary serpentinite studied. The finer-grained serpentinite sandstones are also enriched in discrete magnetite and, to a lesser extent, Cr-Al spinel grains. These phases commonly form thin "trails" parallel to bedding. Mafic volcanic fragments are less abundant (< 1-2%) in these sandstones. Minor components in serpentinite clasts of all sizes include (?) brucite, chlorite, talc, hematite, limonite, cross-fibre chrysotile and anthophyllite. Rare discrete detrital grains of anthophyllite also occur in some samples (e.g. 276).

Chemistry

The bulk chemistry of these sedimentary serpentinites (Table 5.2) strongly reflects their almost exclusively ultramafic provenance. The enrichment in Fe in the finer-grained sandstones (analyses 1,2, Table 5.2) relative to the coarser-grained examples (analysis 3, Table 5.2), and relative to the Watchimbark serpentinites (analyses 4-6, Table 5.2),

---

* Microprobe analyses of these cements fall within the following ranges: SiO_2, 43%-45%; Al_2O_3, 0.3%-0.7%; ΣFe_2O_3, 2.4%-3.2%; MgO, 37.1%-40.3% (*cf.* representative analyses of serpentines in Dungan, 1979b). They are depleted in Ni and Cr (<0.1%) relative to serpentines in coexisting rock fragments and in peridotites generally, and are depleted in Al_2O_3 relative to common bastites after orthopyroxene (0.5%-5% Al_2O_3, unlisted analyses, this study; Dungan, 1979b).

TABLE 5.2

Chemical Analyses and Normative Mineralogy of Sedimentary Serpentinites and associated Watchimbark Serpentinites

	Sedimentary Serpentinites			Watchimbark Serpentinites		
ANALYSIS No.	1	2	3	4	5	6
SAMPLE	430	431	432	433	434	435
SiO_2	46.91	46.44	49.12	46.79	47.58	47.92
TiO_2	0.03	0.04	0.03	0.03	0.01	0.01
Al_2O_3	1.41	1.27	0.68	1.29	0.14	0.26
Cr_2O_3	0.33	0.37	0.32	0.38	0.18	0.26
ΣFeO	9.13	8.63	6.94	7.46	6.65	6.62
NiO	0.27	0.33	0.41	0.31	0.35	0.35
MnO	0.07	0.10	0.10	0.10	0.12	0.09
MgO	41.06	42.24	41.26	42.66	44.16	44.37
CaO	0.22	0.06	0.07	0.06	0.04	0.04
Na_2O	0.02	0.05	0.03	0.03	0.04	0.02
K_2O	0.01	0.01	0.02	0.01	0.01	0.01
P_2O_5	0.04	0.03	0.02	-	-	0.01
TOTAL	99.50	99.57	99.00	99.12	99.28	99.96
ΣVol [1]	12.03	12.49	12.32	12.18	12.96	11.93
FeO[1]	2.51	2.79	0.78	1.59	0.05	1.54
Mg*	88.9	89.6	91.3	91.0	92.1	92.2
CATION NORM						
PL	1.7	1.4	-	-	-	-
CPX	-	-	-	-	-	-
OPX	38.1	34.5	51.7	40.7	37.8	39.6
OL	59.9	63.7	47.5	58.3	62.2	59.8
SP	0.3	0.4	0.8	1.1	-	0.6
TRACE ELEMENTS[2] (µg/g)						
B	n.d.	<10	10	n.d.	n.d.	<10
F		220	230	n.d.	n.d.	170
Cl		200	500	n.d.	n.d.	100
Li		3.2	8.8	-	-	-
Sr		<1	2	-	-	-
Zr		2	5	-	-	-
Nb		<3	3	-	-	-
Y		<2	3	-	-	-
Ti		211	220	170	63	66
Cu		17	9	15	3	2
Zn		51	46	43	40	29
Ni		2595	3248	2474	2748	2728
Co		116	106	108	128	107
V		51	39	41	3	8
Cr		2498	2161	2574	1212	1810
Na		331	251	202	304	179
K		74	142	84	66	53

[1] See Appendix G

[2] Rb,Ba,REE below detection limit

n.d. = not determined

$Mg^* = 100(Mg+Ni)/(Mg+Ni+\Sigma Fe+Mn)$

Major element analyses are recalculated to original totals on a volatile-free basis. Trace element values are also recalculated on a volatile-free basis.

Analyses: 1,2= fine serpentinite sandstone
3= coarse " "
4,6= serpentinized harzburgites ;(5= cumulate?)

is a function of the increased modal abundances of detrital magnetite (Fe_3O_4) (± Cr-Al spinel) in the former. However, the reason for the relative Si-enrichment in the coarse serpentinite sandstones (analysis 3, Table 5.2) is unclear. It is unlikely that the Si-enrichment in this sample reflects a relatively high modal abundance of serpentinized orthopyroxene because; (i) this is not evident petrographically, and (ii) serpentine pseudomorphing orthopyroxene typically retains much of the Al_2O_3 of the host pyroxene (e.g. Dungan, 1979b; unlisted analyses, this study) but the Si-rich sandstone is in fact depleted in Al_2O_3 relative to the other sedimentary serpentinite samples (Table 5.2).

Broad-beam microprobe scans over a number of microlitic volcanic fragments in the sedimentary serpentinite (analyses not listed) indicate that these fragments have been strongly depleted in CaO (< 0.5%) and alkalis (not detected), somewhat less depleted in Al_2O_3 (8%-4%) and enriched in MgO (23%-29%). Most contain 1%-2% TiO_2 and their opaque oxides are titanomaghemites. Comparison of the whole-rock analyses of these sedimentary serpentinites with other PBOC serpentinized peridotites (Tables 5.1,5.2) clearly supports petrographic observations (see above) that the volcanogenic component of these sandstones is quite minimal. As might be expected (*cf.* Dostal *et al.*, 1977) the sedimentary serpentinite is enriched in Li and Cl relative to other PBOC serpentinized peridotites, presumably as a result of chemical interaction with seawater. However, B, which may be extracted into serpentinites from seawater (Thompson and Melson, 1970), F, and alkalis are not noticeably enriched in these sediments. In fact B abundances in the PBOC sedimentary serpentinite (~10 µg/g) are substantially lower than those in oceanic serpentinites (~70-100 µg/g; Thompson and Melson, 1970; Seitz and Hart, 1973). The anomalous enrichment in P_2O_5 (wt %) in the PBOC sedimentary serpentinite might be at least partly due to a biogenic component in these rocks. Furthermore, a residue of carbon remained after dissolution of the sedimentary serpentinite samples and this too is probably largely biogenic in origin.

Fossils

The PBOC sedimentary serpentinite contains an Early Permian (Allandale or Fauna II age, *cf.* Runnegar, 1967; Runnegar and McClung,

1975) sublittoral fauna which includes internal and external moulds of *Eurydesma cf. playfordi*, *Merismopteria* sp., *Keenia* sp. *Peruvispira* sp., *Myonia morrisi* (B. Runnegar, pers. comm.) and an unidentified bivalve mollusc (Plate 5.3B). With very few exceptions (e.g. Plate 5.3A) the bivalve molluscs (including Eurydesma) are articulated (Plate 5.3B) but more-or-less randomly oriented. This might suggest that deposition of their host sediments occurred in an environment fairly proximal to the preferred high-energy life environment of these molluscs (*cf.* Runnegar and Campbell, 1976; Runnegar, 1978).

Provenance

Two principal lines of evidence suggest that the sedimentary serpentinite was derived predominantly from its host, the Watchimbark Serpentinite:

(1) All of the sedimentary serpentinite samples examined contain a significant proportion (*ca.* 10%-30%) of clasts in which the serpentine displays only a bladed, interpenetrating texture similar to that which is characteristic of antigorite (Plate 5.3E, *cf.* Fig. 5c of Wicks and Whittaker, 1977). However, X-ray diffraction scans of a number of bulk samples (260 - 272, 430 - 432) failed to confirm the presence of antigorite in these rocks. The Watchimbark Serpentinite is the only PBOC peridotite which contains some serpentinite displaying this texture (e.g. samples 433, 435, Plate 5.3F) and similar (lizardite) XRD characteristics.

(2) Discrete Cr-Al spinels in the matrix of the sedimentary serpentinite and those occurring in serpentinite clasts are essentially unzoned* but both types display extreme overall variation in their chemical compositions (Figs 5.3,5.4, Table C-10). In fact, of the PBOC serpentinites

---

* Many Cr-Al spinels in these rocks contain overgrowths of secondary maghemite and/or magnetite. This, and the occurrence of thin maghemite rims on some clasts, would suggest that at least some serpentinization occurred in these rocks following deposition.

only the Watchimbark mass contains significant volumes of serpentinized peridotites (cumulate harzburgites and tectonized harzburgites, see Section 5.2) whose Cr-Al spinels display a range of *Cr*-values which is in any way comparable to the range displayed by the detrital Cr-Al spinels (Fig. 5.3d). Nevertheless, serpentinite fragments displaying well-preserved cumulus textures (Plate 5.3G) and tectonite textures (Plate 5.3H) are relatively rare in the sedimentary serpentinite.

In addition, with the exception of several blocks of serpentinite which have been largely replaced by carbonate,* the central portion of the Watchimbark Serpentinite is significantly oxidized compared with all other PBOC serpentinized peridotites (see Section 5.2). This would suggest that it has experienced a more intense and/or more protracted weathering history than the other PBOC serpentinites, and reinforces the suggestion that it may have been exposed to (subaerial ?) weathering and erosion during Early Permian times. The sedimentary serpentinite might be a fragment of a clastic apron surrounding an emergent Watchimbark Serpentinite emplaced during formation of the graben-like structures now occupied by the Manning Group. Because the basaltic clasts in the sedimentary serpentinite contain abundant titanomaghemite they were not derived from the PBOC basaltic suite (see Section 5.7). They may well have been derived from basaltic members of the Woolomin Association. However, relative to basaltic rocks in the Tamworth Belt, for instance, Woolomin (and Myra) basaltic rocks are perhaps insufficiently distinctive

---

* Massive blocks (dimensions of tens of metres or more) of cryptocrystalline- and rare sparry calcite (identified by chemical analysis) in which relict schistose serpentinite textures are exceptionally well preserved (e.g. 258) occur in schistose serpentinite at GR 691,890 and ~GR 755, 869. A discrete horizon of similar material (259) crops out near GR 690, 826 (see Map 1). These rocks are of enigmatic origin. They are not ophicalcite breccias (*cf.* Bonatti *et al.* 1974; Barrett and Spooner, 1977; Knipper, 1978) but rather they appear to have originated *via* highly efficient replacement of the serpentine component of schistose serpentinite by calcite.

in their petrography, mineralogy or chemistry (see Chapter 3) for this to be demonstrated with any confidence. The sedimentary serpentinite may have been emplaced along with Watchimbark serpentinites mobilized from below the zone of weathering during post-Early Permian tectonic events which deformed the Manning Group (see Chapter 1).

5.4 CUMULATE OLIVINE NORITES

5.4.1 Field Relations

Olivine norites (including rare olivine gabbronorites e.g. 459, 480) are the most widespread cumulate rocks in the PBOC. They occur; (i) as relatively small (dimensions of metres or less), isolated, and often partially fragmented tectonic inclusions in highly schistose serpentinite (Plate 5.1E; e.g. localities 1 and 2, Fig. B-1); (ii) as localized clusters of tectonic inclusions (dimensions of tens of metres or less) in a matrix of highly schistose serpentinite (see Fig. B-1), and (iii) as substantial outcrops (dimensions of hundreds of metres or more) adjacent to, structurally overlying (?), serpentinized peridotites (localities 3 and 11, Fig. B-1). All of these examples are fault-bound and no intrusive contacts are preserved. Internally, the more substantial occurrences are considerably disrupted by faulting, shearing and macroscopic-scale brecciation. Continuous, undisturbed outcrops larger than several tens of square metres are rare.

In hand-specimen and in outcrop most PBOC olivine norites display diffuse igneous lamination (Plate 5.4A) or, less commonly, fine-scale layering (Plate 5.4B,C). Where present, thin, (< 1 cm) sharply defined layers (laminae) are almost invariably saussuritized norite or leuconorite assemblages (plag > 50% + opx < 50% ± a trace of sp, cpx, ol) and they rarely constitute more than 5 vol.% of any particular outcrop. On occasion these thin laminae may be highly planar, (Plate 5.4B) but lenticular (Plate 5.4C) and isolated-lensoidal (Plate 5.4D) types* are the most common laminae types. In rare instances, tight, mesoscopic, small amplitude, disharmonic folds (Plate 5.4E) occur in individual

---

* The destruction of several outcrops has revealed that, in overall shape, these lenticules and lenses resemble flattened discs or flattened ellipsoidal discs.

laminae (one observation at each of localities 9 and 11). These extremely localized folds presumably reflect minor, essentially subsolidus plastic flowage (slumping?) which, in turn, might suggest that the cumulates concerned initially crystallized on a significantly inclined surface.

Almost all olivine norites in the PBOC are partially serpentinized (see Section 5.4.2). In addition, a large proportion of the olivine norites at locality 3 and a lesser proportion of those at locality 9 are partially- to highly amphibolitized and saussuritized (see Section 5.4.2). On occasion, olivine norite outcrops at other localities (e.g. locality 5) are similarly altered. Field and petrographic observations on these rocks (*cf.* Section 5.4.2) suggest that: (i) amphibolitization and saussuritization occurred at relatively elevated temperatures in response to the introduction of volatiles *via* shear zones (high-T shears); and (ii) subsequent shear stress at lower temperatures produced extensive low-T (no recrystallization) shearing which may be localized within high T (amphibolitized) shears, but is typically more widespread.

At locality 3 a thick carapace of almost pervasively sheared (low-T), highly amphibolitized olivine norites structurally overlie less-altered and rare fresh equivalents (Map 1, Fig. 5.1). High-T and low-T shear zones also occur within the less-altered rocks, and of these, relatively discrete amphibolitized zones typically range from less than one metre to perhaps ten metres in width. These crop out poorly although microscopic and mesoscopic high-T shears (Plate 5.4F,G) are typically abundant in the adjacent olivine norites. At most localities low-T shearing predominates and only fragments of amphibolitized zones are found (e.g. locality 9). Some amphibolites in these zones are exceedingly coarse-grained (Plate 5.4H) and individual prismatic magnesiohornblende crystals may exceed 25 cm in length.

5.4.2 Petrography

Primary Textures

Modal abundances of primary phases in the majority of PBOC olivine norites fall in the following ranges; olivine 10%-60%, orthopyroxene 20%-45%, plagioclase 10%-50%, clinopyroxene <1%-10% and Cr-Al spinel 0.5%-1.5%. For the most part they are strictly olivine mela-norites in

PLATE 5.4

Layering and Mesoscopic Alteration in PBOC Olivine Norites

A. Diffuse igneous lamination in PBOC olivine norite. White grains are saussuritized plagioclase [GR7140,9200; locality 11, Fig. B-1].

B. Fine-scale semi-continuous planar layering in PBOC olivine norite. Thin sharply-defined laminae are typically leuco-norite assemblages. Hammer handle is approximately 3.5 cm in diameter [GR6500,8125; locality 3, Fig. B-1].

C. Thin lenticular leuco-norite laminae in PBOC olivine norite. The larger of the white patches are lichen, the remainder are coarse-grained saussuritized plagioclase [GR6495,8130; locality 3, Fig. B-1].

D. Isolated-lensoidal leuco-norite lamina in PBOC olivine norite. Large irregularly-shaped white patches are lichen [GR7150,9185; locality 11, Fig. B-1].

E. Mesoscopic disharmonic folds in a plagioclase-rich lamina in PBOC olivine norite. Sketch illustrates the approximate original form of the folds prior to sampling. Left (highly oblique) face of specimen is 10-11 cm in height [sample 332, GR8230,8620; locality 9, Fig. B-1].

F. Sub-mesoscopic amphibolitized microshears (black) in PBOC olivine norite. Note saussuritization of plagioclase (white grains) immediately adjacent to these shears. Plagioclase is more-or-less homogeneously distributed throughout this sample. Thin section is 14.5 cm x 10 cm, photographed under incident light [sample 322, GR6490,8135; locality 3, Fig. B-1].

G. Mesoscopic amphibolitized shears (relatively pale coloured) in PBOC olivine norite. Pen is 15 cm in length [GR7220,8635; locality 9, Fig. B-1].

H. Extremely coarse-grained prismatic magnesiohornblende in completely amphibolitized PBOC olivine norite. Pen is 1.5 cm in diameter Moss and lichen cover much of the field of view [GR7150,8685; locality 10, Fig. B-1].

PLATE 5·4

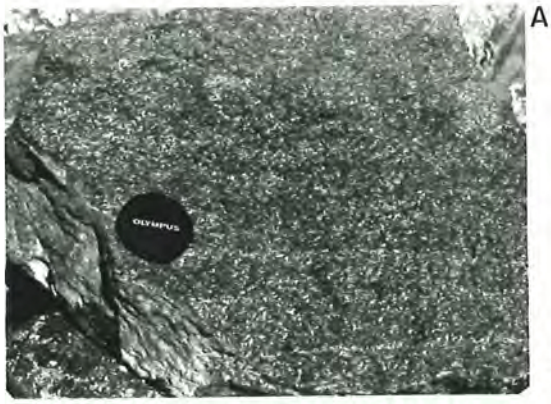

A

B

C

D

E

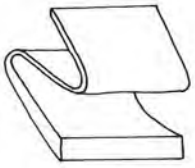

F

G

H

the terminology of Streckeisen (1976) (see footnote in Introduction, Part II) and they are invariably devoid of primary phases other than the five listed above. In general, normative (and modal) abundances of primary phases vary more-or-less systematically. Thus PL and, to a lesser extent, CPX increase regularly with increasing OPX and decreasing OL (Fig. 5.2) and SP.

The PBOC olivine norites typically display adcumulus or rarely heteradcumulus (poikilitic) textures. With the common exception of clinopyroxene, which usually displays postcumulus or intergranular habits (Plate 5.5A), all primary phases in these rocks may occur as discrete cumulus phases with or without obvious postcumulus overgrowths*, and as comparatively small intergranular postcumulus growths (intercumulus grains), all within a single thin-section (Plate 5.5A-C). In some instances these 'intercumulus grains' simply might be small outgrowths of larger grains, the bulk of which were originally situated above or below the plane of the thin-section. Approximately 140 thin-sections from ~105 olivine norite samples were examined in detail. None of these display petrographic (or other) evidence for the crystallization of trapped interprecipitate liquid (*cf.* ortho- and mesocumulates; Wager *et al.*, 1960).

Grainsizes of primary phases in the PBOC olivine norites may range from 5 mm to 0.05 mm or less within single samples (e.g. 519). However, most grains in most samples fall within the size range 3 mm - 0.1 mm. Cr-Al spinels are typically opaque, euhedral and are most conspicuous ($\lesssim$ 0.3 mm) in the olivine-rich variants (e.g. 479). They also occur in the olivine-poor types (e.g. 440) where they may be as small as 0.02 mm. In all PBOC olivine norites Cr-Al spinel displays a discrete intergranular habit and also occurs as inclusions in olivine, orthopyroxene, plagioclase and, on occasion, clinopyroxene. All silicates may contain inclusions of, or form inclusions in, any or all of the others (e.g. 443, 445). Ortho-

---

* In this context, 'outgrowths' is perhaps better terminology than 'postcumulus overgrowths' because in these PBOC rocks, and possibly in most adcumulates, it is unlikely that there was a significant hiatus (temporal, spatial or, in this case at least, chemical) between the growth of the bulk of a crystal in "free space" and the growth of its more remote extremities in "confined space" (see text and *cf.* McBirney and Noyes, 1979).

pyroxene inclusions in plagioclase, however, are relatively rare. The overall textural relationships displayed by primary phases, and in particular the relative abundances of cumulus phases which display minimal evidence of outgrowth compared with their overall size, suggest that the crystallization sequence in the PBOC olivine norites was Cr-Al spinel (sp) → sp + olivine (ol) → sp + ol + orthopyroxene (opx) → sp + ol + opx + plagioclase (pl) → sp + ol + opx + pl + clinopyroxene. With the possible exception of at least one heteradcumulate (464) which contains abundant olivine euhedra included in large (up to 5 mm) poikilitic ortho- and clinopyroxenes (Plate 5.5D), and contains postcumulus plagioclase (only; Plate 5.5E), it would seem that spinel, olivine, orthopyroxene and plagioclase appeared within a small near-liquidus temperature interval, and then continued to crystallize throughout the entire crystallization history of these cumulates. This crystallization history is discussed further in the discussion following Section 5.4.4.

At least some, but by no means all, orthopyroxenes in most samples contain subsolidus* exsolution lamellae or blebs of Ca-rich pyroxene and discrete Ca-rich pyroxenes usually contain thin slivers or partial lamellae of exsolved Ca-poor pyroxene. Silicates in many olivine norites display slight or moderate strain extinction although a number of samples (e.g. 440) are essentially unstrained.

Secondary Textures

Secondary phases include; serpentinite + magnetite, magnesio-hornblende, hydrogarnet, prehnite, sericite, Al-rich spinel (pleonaste) and rare chlorite. Serpentinization of olivine and, to a lesser extent, orthopyroxene and saussuritization (hydrogarnet ± prehnite ± sericite ± (?) clay minerals) may be significant in comparatively undeformed olivine norites. However, the development of secondary amphibole is largely restricted to sheared examples. Saussuritization of plagioclase is also generally more advanced in the vicinity of the high-T shear zones and this is well illustrated on a sub-macroscopic scale in Plate 5.4F. Adjacent to the high-T shear zones, plagioclase and pyroxenes are partially

---

* These lamellae equilibrated with their host orthopyroxenes at temperatures similar to discrete opx-cpx pairs (i.e. 800°C-1050°C; see Appendix D).

PLATE 5.5

A. Postcumulus clinopyroxene (Cp) in olivine norite cumulate. Note blebs of Ca-poor pyroxene exolved from the clinopyroxene. O = olivine, Op = orthopyroxene, P = plagioclase, A = secondary fibrous amphibole [sample 438, mag. = 35x , crossed nicols].

B. Cumulus olivine (large central dark-grey grain) displaying adcumulus overgrowths ('outgrowths', see p206) in PBOC olivine norite. Grains displaying cleavage are orthopyroxene. With the exception of small equigranular olivines displaying typical fracturing (lower right), the remaining grains are plagioclase and accessory Cr-Al spinel (examples arrowed).[sample 440, mag. = 22x , crossed nicols].

C. Postcumulus olivine + plagioclase + orthopyroxene (see below) in PBOC olivine norite. All these grains are optically continuous and chemically homogeneous, including the intergranular orthopyroxene (O) and its ribbon-like outgrowth [sample 438, mag. = 35x , crossed nicols].

D. Partially serpentinized olivine (dark) and Cr-Al spinel euhedra (examples arrowed) poikilitically included in part of a coarse-grained orthopyroxene (white) heterad in a PBOC plagioclase-poor olivine mela-norite heterad-cumulate [sample 464, mag. = 22x , crossed nicols].

E. Highly cuspate postcumulus saussuritized plagioclase pseudomorphed by hydrogarnet (black) in a plagioclase-poor olivine mela-norite heterad-cumulate. Cumulus grains are partially serpentinized olivine with small Cr-Al spinel inclusions (black euhedra). [sample 464, mag. = 22x , crossed nicols].

F. Fine-grained bladed and decussate magnesiohornblende replacing plagioclase + pyroxene (relict orthopyroxene = O, partially pseudomorphed clinopyroxene = dark grain, lower left) in highly amphibolitized shear through olivine norite.[sample 325, mag. = 35x , crossed nicols].

G. Pleonaste euhedra (dark grey) in amphibolitized shear through olivine norite. Pale grains are bladed magnesiohornblende [sample 325, mag. = 90x , partially crossed nicols].

H. Coarse-grained interlocking texture in completely amphibolitized olivine norite. Large grains are magnesiohornblende with rare intergranular chlorite (Chl). Some magnesiohornblende displays polysynthetic twinning (upper left).[sample 324, mag. = 22x , crossed nicols].

cf. 5.5C

spinel labradorite bronzite ol olivine

PLATE 5·5

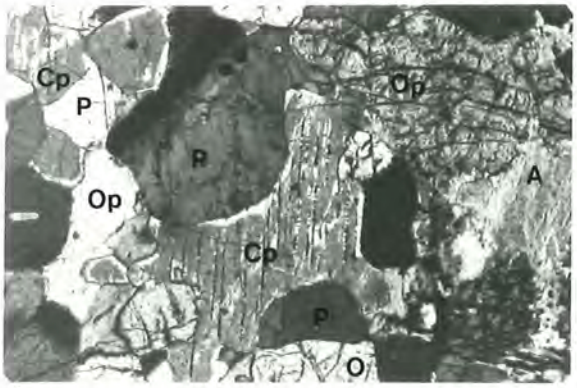

A

B

C

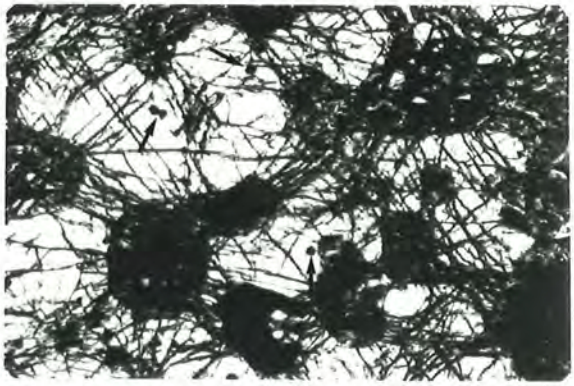

D

E

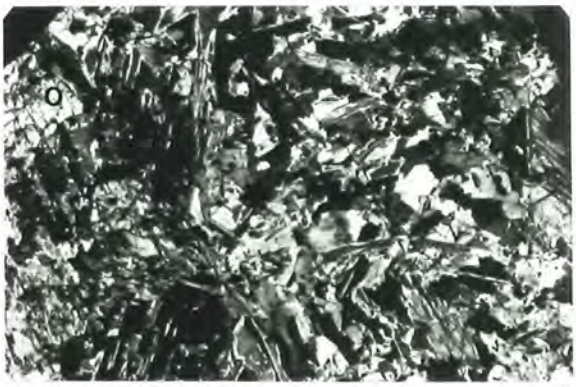

F

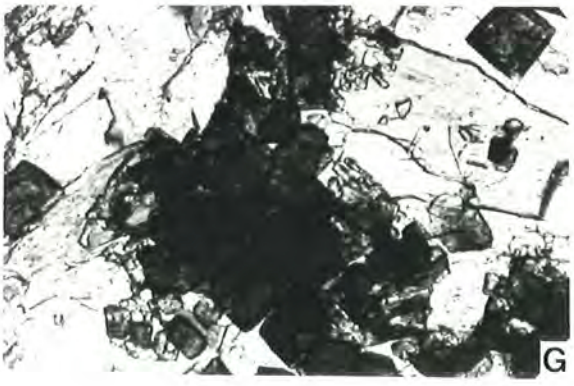

G

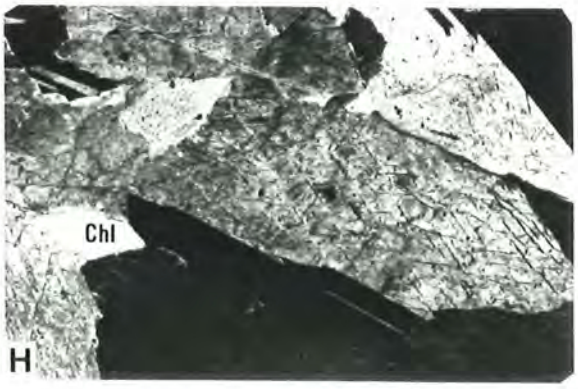

H

replaced by fine, bladed-decussate magnesiohornblende (Plate 5.5F) which may contain discrete or clustered pleonaste euhedra (Plate 5.5G). Pleonaste also forms clusters around relict Cr-Al spinel. The completely amphibolitized horizons may be exceedingly coarse-grained (Plate 5.4H) and consist almost entirely of coarse interlocking grains of green (very pale green in thin-section, deep green-greenish black in hand-specimen) magensiohornblende with minor intergranular chlorite (Plate 5.5H). Patches of bladed chlorite may also be present in some incipiently amphibolitized variants (e.g. 456). The amphibolites may contain sparse fine veins consisting of prehnite, magnesiohornblende ± chlorite, assemblages (e.g. 324). Cataclastic 'veins' and shears are relatively common in these amphibolite horizons (e.g. 327) and magnesiohornblendes in many of the comparatively undisrupted examples (e.g. 324) display strong strain extinction.

5.4.3 Mineral Chemistry

Perhaps the most striking feature of the mineral chemistry of the PBOC olivine norites is the virtual absence of compositional zoning in the primary phases. In general the cores of the larger cumulus grains are essentially identical in composition to the rims of analogous post-cumulus 'scraps'. Furthermore, very detailed investigations of the compositions of Cr-Al spinels in various textural relationships in the olivine norites has revealed, somewhat surprisingly, (*cf.* Henderson, 1975; Henderson and Wood, 1981) that they too display only negligible chemical variation, even between early precipitated grains included in olivine and later intergranular Cr-Al spinels. The absence of cryptic variation within single specimens appears to be a primary characteristic rather than being strictly a function of subsolidus re-equilibration. Thus, spinels totally enclosed in plagioclases are identical in composition to all others in contact with, or included in, ferromagnesian phases.

A general rarity of compositional zoning is a common feature of primary phases in adcumulates (e.g. Wager, 1963), but extreme examples involving 5-phase assemblages (e.g. the olivine norites under discussion) are not well-documented.

Primary Phases

Cr-Al spinels in PBOC olivine norites are unzoned and have *Cr*

values in the range 50-65 and *M* values in the range 15-45 (Tables C-1, C-2). As such, they are somewhat Cr-poor relative to most Cr-Al spinels in stratiform intrusions, ophiolitic gabbros and MORG (Figs 5.3d,5.4). With the exception of some spinels in the Panton Sill, Western Australia (Hamlyn 1975,1980; Hamlyn and Keays, 1979), at a given *Cr* value these PBOC spinels extend to more Fe-rich compositions than spinels in stratiform intrusions (Fig. 5.3d). Cr-Al spinels in the PBOC olivine norites display a general Fe-enrichment trend of decreasing *M* with decreasing Mg^* of the coexisting olivines (Fig. D-1). In Figure 5.3a,b,c this Fe-enrichment trend translates to trends of increasing Ti, V and Fe^{3+} (respectively) with increasing Fe-enrichment. In general, the compositions of Cr-Al spinels in the PBOC plagioclase-bearing peridotites are comparable to those of spinels in the olivine norites (Fig. 5.3). Overall, the latter display more significant (primary) Fe^{3+}-enrichment in their more Fe-rich variants than do analogous spinels in stratiform intrusions (Fig. 5.3c) but their overall Fe^{3+}-enrichment is less than that of Rhum spinels, for instance (*cf.* Fig. 7 of Mussallam *et al.*, 1981). Nevertheless, the relatively high Fe^{3+} (calculated) contents of Cr-Al spinels in samples 440 and 441 (~22% calculated Fe_2O_3; page 1 of Table C-2) are strongly at variance with the exceptionally low whole-rock Fe_2O_3/FeO ratios of the host rocks (0.07, 0.08 respectively; analyses 1 and 2, Table B-3).

Olivines display only relatively restricted variation in Fo ($Fo_{86.5-80.5}$, Table C-2) and olivine Fe-Mg variation (~± $Fo_{0.2}$) within most individual samples is perhaps less than the reliable precision limits of the microprobe. NiO and MnO fall in the ranges 0.36%-0.19% and 0.22%-<0.09% respectively and, in general, MnO increases with decreasing Fo (Table C-2). However, NiO varies irregularly as a function of Fo. CaO is always below the microprobe detection limit (<0.07%).

Orthopyroxenes are consistently relatively magnesian bronzites (81 < *mg* < 87, Table C-1, Fig. 5.5) with low to moderate *Ca* values (1-5, Fig. 5.5; CaO falls in the range 0.7%-2.5%; mean = 1.2%, standard deviation = 0.4). Most analyses listed (Tables C-2,C-3) are averages of several grains which are essentially devoid (at least in the portion thin-sectioned) of an exolved Ca-rich phase. In general, however, these grains are only slightly more Ca-rich compared with coexisting orthopyroxenes containing exolved Ca-rich pyroxene. In some samples (e.g. 461,

467), especially some olivine gabbronorites (e.g. 459, 480), orthopyroxene rims are significantly depleted in Ca relative to their cores (Table C-3), but the majority of orthopyroxene grains is relatively homogeneous with respect to Ca.

The Al_2O_3 and Cr_2O_3 contents of orthopyroxenes largely fall in the ranges 1.6%-2.5% (mean = 1.9%) and 0.2%-0.6% (mean = 0.4%) respectively. TiO_2 is below the microprobe detection limit (<0.07%). With increasing *mg*, Cr_2O_3 tends to gradually increase but Al_2O_3 remains relatively constant (Fig. 5.6a,b). For the most part, grains whose rims are depleted in Ca (Table C-3) display similar zoning trends with respect to Al and Cr (Fig. 5.6a,b). However, core and rim compositions of the zoned orthopyroxenes typically fall within the overall compositional ranges displayed by their unzoned analogues (Fig. 5.6a,b).

Clinopyroxenes are diopsides displaying a rather limited range of *Ca:Mg:Fe'* (Fig. 5.5) and a restricted range of *mg* values (86-90, Table C-1). On average, they are significantly more Ca-rich than their counterparts in the PBOC plagioclase-bearing peridotites. However they contain less Ca than the majority of Ca-rich pyroxenes in the PBOC tectonized harzburgites (Fig. 5.5).

With the exception of an anomalously Al-rich variant (463, 3.7% Al_2O_3), the clinopyroxene Al_2O_3 and Na_2O contents fall in the ranges 2.3%-3.0% and <0.3% respectively, and remain relatively constant as *mg* varies (Fig. 5.6c, Table C-1). However, in common with their coexisting orthopyroxenes, the average Cr_2O_3 in these diopsides increases gradually with increasing *mg* (from 0.6% to a maximum of 1.1%, Fig. 5.6d). Several samples (459, 467, 470) contain normal- or reverse-zoned diopsides whose rims are relatively depleted in Al_2O_3 and Cr_2O_3 (Fig. 5.6c,d). Diopsides in the olivine norites consistently contain less than 0.1% TiO_2 and diopsides in each sample average <0.07% TiO_2.

Plagioclases are calcic bytownites (An_{90-85}; Table C-1) or rarely anorthites (e.g. 467). They display only slight compositional heterogeneity ($\pm An_1$) which in large part might simply reflect microprobe analytical constraints in Na determinations. Plagioclases are relatively depleted in Mg (MgO < 0.09) and contain significantly less Fe (ΣFeO < 0.3%) than plagioclases in the PBOC low-Ti gabbros (see Table C-5).

Secondary Phases

Secondary amphiboles are typically Mg-rich magnesiohornblendes or, on occasion, tremolitic hornblendes (Table C-6). In common with their hosts they are highly depleted (< 0.07%) in TiO_2 and K_2O. The Si, Al and Na components of coexisting amphiboles may vary considerably (e.g. analyses 6 and 7, Table C-6) but relatively Al- and Na-rich (9%-12% Al_2O_3, 1%-2% Na_2O) types predominate. For the most part they possess relatively low Al^{VI}:Si ratios and hence they most probably crystallized at pressures somewhat less than 5kb (Fig. 5.8). Most have Al^{VI} comparable to similar secondary amphiboles in one of the plagioclase-bearing peridotites and Al^{VI} is also comparable to primary tschermakitic hornblende in PBOC amphibole-bearing harzburgite (Fig. 5.8). All amphiboles in PBOC intrusives contain less than 0.1% chlorine.

Hydrogarnets in the PBOC olivine norites and plagioclase-bearing peridotites are generally hydrogrossulars with highly variable hydro-andradite and (?) hydropyrope components (Table C-8; *cf.* analyses in Hutton, 1943; Baker, 1959; Ford, 1970; Honnorez and Kirst, 1975). Prehnites, on the other hand, are relatively Fe-poor (Table C-8, analyses 17-20). Some saussuritized 'plagioclasite' lenses (centimetre-scale) consisting almost entirely of hydrogarnet with minor prehnite sericite and relict Cr-Al spinel may be anomalously enriched in K_2O (e.g. 0.4%, Table C-8, analysis 2). Metamorphic spinels in the amphibolitized olivine norites are highly aluminous (61%-65% Al_2O_3) Cr-bearing (<4% Cr_2O_3) pleonastes (Table C-7) and the accessory chlorites are Cr-bearing (<0.4% Cr_2O_3) sheridanites [e.g. $(Mg_{8.3}Al_{2.3}Fe_{1.4})(Si_{5.5}Al_{2.5})O_{20}(OH)_{16}$; sample 324].

5.4.4 Whole-Rock Chemistry

One or more representative samples of olivine norite from each of localities 1-3 and 5-12 (Fig. B-1) have been chemically analysed and these analyses are listed in Appendix B. In particular, the chemistries of all olivine norite variants at the two principal localities (localities 3 and 11, Tables B-3 and B-6 respectively) are examined and representative analyses of these rocks are listed in Table 5.3.

The PBOC olivine norites are quite unusual and, for the moment, perhaps unique in several aspects of their chemistry. Although they

TABLE 5.3

Selected Major and Trace Element Analyses of Olivine Norites from the PBOC

ANALYSIS No.	1	2	3	4	5		6
SAMPLE	440	443	456	467	$\bar{x}$	s	531
SiO_2	49.64	48.34	45.88	43.28	48.24	0.86	47.90
TiO_2	0.05	0.04	0.03	0.02	0.04	0.01	0.03
Al_2O_3	13.13	10.66	8.17	4.86	9.02	1.11	18.44
Cr_2O_3	0.28	0.45	0.70	0.69	0.45	0.03	0.32
Fe_2O_3	0.52	0.55	0.65	0.74	0.59	0.03	0.26
FeO	7.40	7.93	9.31	10.64	8.39	0.40	3.74
NiO	0.05	0.10	0.15	0.19	0.10	0.01	0.04
MnO	0.16	0.18	0.20	0.21	0.19	0.01	0.11
MgO	19.48	23.71	29.94	36.60	26.28	1.27	14.62
CaO	8.59	7.63	4.97	2.72	6.27	0.56	13.70
Na_2O	0.58	0.40	0.25	0.08	0.31	0.13	0.36
K_2O	0.02	0.04	0.04	0.01	0.02	0.01	0.11
P_2O_5	0.01	-	0.01	0.01	0.02	0.01	0.02
TOTAL	99.91	100.03	100.30	100.05	99.92		99.65
ΣVol[1]	1.20	3.54	5.61	9.90	3.68	1.03	2.94
FeO[1]	7.38	6.18	7.24	5.48	6.91	1.28	n.d.
Mg^*	81.2	83.1	84.1	85.0	83.7	0.2	86.5
CATION NORM							
PL	34.5	26.9	19.9	10.6	22.0	3.3	49.2
CPX	8.2	9.1	3.8	1.0	8.0	0.4	18.3
OPX	44.6	38.5	29.7	19.9	40.4	5.5	18.4
OL	12.5	25.0	45.4	67.2	29.0	4.9	14.0
SP	0.3	0.6	1.2	1.3	0.7	0.1	0.1
TRACE ELEMENTS µg/g							
Cu	28	19	19	7	18	8	21
Zn	59	55	42	47	53	7	31
Ni	430	754	1144	1529	751	68	284
Co	75	90	104	114	97	11	86
V	96	96	82	54	98	10	56
Cr	1906	3059	4766	4717	3109	191	2167

[1] See Appendix G. (Fe_2O_3/FeO adjusted to 0.07 = measured Fe_2O_3/FeO, sample 440)

$Mg^* = 100(Mg+Ni)/(Mg+Ni+\Sigma Fe+Mn)$, n.d. = not determined

Analyses 1-4 = olivine (mela)-norites, locality 3; Analysis 5 = mean of 8 olivine (mela)-norites, locality 11; s = standard deviation; Analysis 6 = relatively plagioclase-rich variant, locality 3.

Major element analyses are recalculated to original totals on a volatile-free basis. Trace element values are also recalculated on a volatile-free basis.

For analyses 1-5: Rb < 1 µg/g and Ba, Sr, Zr, Y < 5 µg/g.

For analysis 6: Rb = 2, Ba = 19 and Sr = 107 (µg/g).

display a degree of Fe-enrichment (4% < ΣFeO < 11%) comparable to that in MORG and most ophiolitic gabbroic rocks (*cf.* Beccaluva *et al.*, 1979; Serri, 1981), this Fe-enrichment takes place over an extremely restricted range of ΣFeO/MgO values (0.2-0.4, Fig. 5.10). Furthermore, relative to the great majority of MORG and ophiolitic "gabbros", the PBOC olivine norites are exceedingly depleted in TiO_2 (<0.1% average TiO_2 = 0.03%; Fig. 5.10), incompatible and large ion lithophile minor and trace elements, and LREE. In fact, Rb, Ba, Sr, Zr and Y abundances in these PBOC intrusives are generally less than 5 µg/g (< 10 µg/g in the case of Sr) in all but the more altered examples (Appendix B, note analyses in Table B-7), and P_2O_5 rarely exceeds 0.02 wt%. LREE (La, Ce and Nd) abundances are always below the detection limits of the XRF instrument used (< 2 µg/g for 800 sec. counting time). In fact, La, Ce and Pr abundances in the freshest, most 'evolved' olivine norite (440, Mg^* = 81) are below the detection limits of routine mass spectrometry techniques (Fig. 5.11) and the overall REE pattern of this rock compares more closely with those of oceanic and ophiolitic depleted peridotites than with oceanic and ophiolitic 'gabbroic' cumulates (*cf.* Frey, 1970; Masuda and Jibiki, 1973; Kay and Senechal, 1976; Menzies *et al.* 1977; Hedge *et al.*, 1979; Suen *et al.*, 1979; Tiezzi and Scott 1980; Pallister and Knight 1981).

Sample 440 displays a slight positive Eu anomaly (Fig. 5.11). Because its Ca-rich pyroxene is anomalously depleted in Eu (Fig. 5.11), it is more likely that the positive Eu anomaly in the host reflects some plagioclase accumulation. Although this sample is exceedingly depleted in LREE and ΣREE (~1 µg/g), it is significantly and, for the present, inexplicably enriched in radiogenic Sr (initial $^{87}Sr/^{86}Sr \approx 0.704$-0.705, see Table H-2) relative to values which might be expected (? less than

0.703) by analogy with other relatively 'depleted' basaltic and gabbroic rocks (e.g. Hedge *et al.*, 1979; Cohen *et al.*, 1980; Richard and Allegre, 1980). It must be re-emphasized that this rock is exceptionally fresh and it is extremely unlikely to have been enriched in ^{87}Sr by secondary processes (*cf.* Hart *et al.* 1974). Furthermore, its constituent unaltered primary phases (cpx, opx and plagioclase) are also enriched in ^{87}Sr ($^{87}Sr/^{86}Sr$ ~0.7045-0.705, see Appendix H).

Although alkali abundances in many of these rocks have been significantly modified by secondary processes (see Appendix A, and compare, for instance, analyses of samples 440 and 326 which are from the same outcrop, Tables B-3 and B-7 respectively), several lines of evidence suggest that the PBOC olivine norites are intrinsically highly depleted in K and, to a lesser extent, Na. These include: (i) the low Na_2O and K_2O contents of the freshest and, coincidentally, most evolved sample analysed (Na_2O = 0.58%, K_2O = 0.02%; Analysis 1, Table 5.3 - incipient serpentinization of olivine, other phases remarkably fresh) and, (ii) the general trend of decreasing Na_2O with decreasing PL and increasing Mg^* in olivine norites at locality 3 (Table B-3). Depletion in K and Na is particularly evident if the K_2O and Na_2O contents of samples displaying anomalously high abundances of the relatively mobile trace elements such as Rb, Ba and to some extent, Sr and Li (e.g. 469, 447, 518, 520 Appendix B), and those samples displaying obvious petrographic evidence of alteration (Table B-7) are discounted. Extrapolating from sample 440 (0.58% Na_2O) and paying due regard to the relatively Na- and K-poor chemistries of primary phases (Appendix C), the Na_2O and K_2O contents of even the most plagioclase-rich olivine norite variants (e.g. 531, Table 5.3 - excluding the individual, volumetrically minor leuco-norite laminae; see Section 5.4.1) were probably less than 0.9 and 0.05 wt%, respectively. Bearing in mind the otherwise relatively depleted chemistry of the PBOC olivine norites, and taking into account variation in *mg* values and modal compositions, the PBCC olivine norites have higher Na_2O contents than might be expected, compared with most ophiolitic and oceanic 'gabbroic' and mela-'gabbroic' cumulates (see Coleman, 1977 and Fox and Stroup 1981, for summaries of the chemistries of these rocks). An analogous situation exists with the PBOC low-Ti basalts (see Section 5.7.4).

Relative to oceanic and ophiolitic 'gabbroic' and mela-'gabbroic' cumulates most PBOC olivine norites are significantly enriched in Ni (400-1600 µg/g) and Cr (2000-5000 µg/g). Many of the olivine norites and most of the plagioclase-bearing peridotites in the PBOC are also notably enriched in Cr relative to the associated tectonized harzburgites (< 2800 µg/g Cr, Table B-1). Indeed, many of the relatively Mg-rich PBOC cumulates (e.g. 460, 470, 472; see Table 5.1 and Appendix B) are enriched in Cr relative to tectonized harzburgites and cumulates from 'similar' ophiolitic and oceanic associations where Cr-Al is also disseminated (*cf.* Irvine and Findlay, 1972; Coleman, 1977; Jaques and Chappell 1980; Bonatti and Hamlyn 1981; Boudier and Coleman 1981; Fox and Stroup 1981; Smewing, 1981). On the other hand, for a given olivine or *ol* content, Ni abundances in the PBOC cumulates are anomalously low when compared with olivine-bearing cumulates in the settings listed above (see below).

Discussion

Although all analysed olivine norites from the various localities in the PBOC are remarkably similar in most aspects of their chemistry (excluding elements such as K and Na which obviously have been mobile to some extent during alteration) and mineralogy, those from localities 3, 11 and 12 display some distinctive chemical characteristics. Thus, relative to analogous olivine norites elsewhere in the PBOC: (i) those at locality 12 (Table B-6) are enriched in TiO_2 (~0.08%) and, to a lesser extent, CPX (~11%); (ii) those at locality 11 are, on average, slightly enriched in SiO_2 and slightly depleted in Ni and Cr (Fig. 5.9), and; (iii) when plotted as functions of the Fo content of their respective olivines, which reflect the *M* values of the melts from which they crystallized (Roeder and Emslie, 1970), the chemistries of most of those at locality 3 vary in a somewhat distinctive fashion (Fig. 5.9). Furthermore, pyroxenes in sample 463 (locality 1) are anomalously enriched in Al_2O_3 relative to those in most other PBOC cumulates (Fig. 5.6).

The above data suggest that the PBOC olivine norites are fragments of a series of discrete but nevertheless consanguineous intrusives rather than relicts of a disrupted single intrusive. Whatever the original dimensions and form of these intrusives, all have been disrupted

and disaggregated to varying degrees by subsequent high- and low temperature shearing. In some respects the PBOC amphibolitized shear zones resemble those found in some MORG (e.g. Helmstaedt and Allen 1977; Malcolm, 1981; Prichard and Cann 1982) but retrograde greenschist facies assemblages usually predominate in the latter (Fox and Stroup 1981). Furthermore, amphibolitized MORG and ophiolitic metagabbros (e.g. Gass and Smewing 1973; Coish, 1977; Hutchison, 1978; Mevel *et al.*, 1978; Stern and Elthon, 1979) are devoid of highly aluminous metamorphic spinel. This suggests that they initially recrystallized at somewhat lower temperatures (< 700°C?) than the pleonaste-bearing PBOC amphibolitized olivine norites (*cf.* Fig. 12 of Matthes and Knauer, 1981; Whitney,1972; Evans, 1977; Coolen, 1981; Harris, 1981). In addition, the low Cl abundances (< 0.1%, perhaps < 0.05%) in the PBOC magnesiohornblendes tend to suggest that sea water was not involved in the amphibolitization process (*cf.* Prichard and Cann 1982). Because PBOC parental magmas appear to have been unusually "dry" (see below), the ultimate source of fluids involved in the high-T metamorphism of the PBOC olivine norites remains enigmatic.

Ophiolites containing significant orthopyroxene in their cumulate sequences are not uncommon. Examples include Troodos (e.g. Greenbaum, 1972) Betts Cove (Gale, 1973; Church, 1977), Khan-Taishir (Zonenshain and Kuzmin, 1978), Papua New Guinea (England and Davies 1973; Jaques, 1981), Tasmania (Brown *et al.* 1980), Oman (Smewing, 1981) and Sabzevar/ Khorassan, Iran (Lensch *et al.*, 1977). However, in addition to certain unusual aspects of their chemistry (see above), the PBOC olivine norites and plagioclase-bearing peridotites are distinctive in that: (i) their crystallization sequence is sp → ol → opx → plag → cpx (*cf.* Church and Riccio 1977; Irvine, 1979); modal opx >> cpx; (ii) throughout the entire sequence, cumulus grains and analogous coexisting postcumulus grains are identical in chemistry; (iii) Cr-Al spinel (Cr ~55-63) crystallized from melts with M values (calculated) as low as ~55 to the exclusion of other Fe-bearing oxides throughout the entire olivine-bearing cumulate sequence; and (iv) late-crystallizing cpx is surprisingly Cr-rich (e.g. in sample 440, postcumulus diopside containing 0.68% Cr_2O_3 coexists with olivine as Fe-rich as $Fo_{80.5}$).

On the basis of available liquid-mineral partitioning relations, and by simple comparison with gabbroic and mela-'gabbroic' rocks in

oceanic and ophiolitic settings (see above) it is evident that the melts parental to the PBOC olivine norites were extremely depleted in incompatible elements such as Zr, Y, Ti, P, REE; in large-ion lithophile elements such as Ba, Sr, Rb; and in K. On the other hand, relative to melts from which somewhat analogous MORG and most ophiolitic cumulates presumably crystallized, these PBOC melts appear to have been enriched in Si (*en*) and Cr, and perhaps Ni (~200-500 µg/g Ni assuming K_D of 6-10 between olivine and melt; Hart and Davis, 1978). Furthermore, the lack of primary hydrous phases and primary magnetite in the PBOC olivine norites, and the exceptionally low Fe_2O_3/FeO ratios (< 0.08; *cf.* Haggerty, 1978) of the fresh examples, suggest that the PBOC parental melts were almost invariably 'dry'. All these characteristics suggest that the parental melts from which these PBOC cumulates were ultimately derived may have originated by high temperature, relatively low pressure (< 5-9kb?) partial melting of an unusually depleted, but perhaps relatively *en*-rich upper mantle source (*cf.* Duncan and Green 1980a; Jaques and Green 1980; Sen, 1982).

However, judging by the range of olivine compositions displayed by the PBOC olivine norites (Fig. 5.9, Table C-2), the *M* values of the melts from which they crystallized were relatively low ($55 < M < 66$, assuming olivine-liquid Fe-Mg $K_D = 0.3$; Roeder and Emslie, 1970). Consequently, melts with these *M* values are unlikely to have been primary melts in equilibrium with depleted, refractory upper mantle. It is for this reason that one is led to suspect that the original cumulate component of the PBOC may have included a range of relatively more Mg- and Ni-rich, and perhaps somewhat Cr-poor (for a given *M* value the PBOC olivine norites are unusually rich in Cr) dunitic or harzburgitic variants (Fo_{92-87}?) whose spinels are relatively Cr-poor. It is tempting to suggest that some of the Watchimbark cumulate harzburgites (e.g. 434, analysis 5, Table 5.2) might be remnants of such a sequence. On the basis of the above discussion, the parent melts to these known and postulated PBOC cumulates might be classified as 'boninitic' or 'low-Ti basaltic' and, to a first approximation, the PBOC low-Ti basalts would appear to be likely candidates. There are, however, some problems with this interpretation (see Section 5.7.4).

The relatively early crystallization of highly calcic plagioclase

(An_{91-85}) in these PBOC cumulates (rapidly following orthopyroxene relative to the rather late appearance of significant clinopyroxene) and the moderate amounts of Al (1.6%-2.5% Al_2O_3) and Ca (0.7%-2.5% CaO) in relatively early-crystallized orthopyroxenes (Figs 5.5,5.6), all suggest that their parent melts were not significantly depleted in Al_2O_3 and CaO. Al- and Ca-depletion might have been expected by analogy with many otherwise comparably depleted basaltic melts such as boninitic, komatiitic, and low-Ti basaltic types (e.g. Sun and Nesbitt 1978; Cameron *et al.* 1979; Francis and Hynes 1979). In fact, these PBOC melts were probably rather Al-rich (> 16% Al_2O_3 ?), the early crystallization of plagioclase also being facilitated by essentially anhydrous conditions (Hamilton *et al.* 1964) which, in turn, necessitate relatively high liquidus temperatures (Duncan and Green 1980a,b). Perhaps crystallization at relatively high temperatures was the principal factor controlling the entry of significant Ca in orthopyroxene (see Section 5.4.3). Only in the comparatively evolved quartz-bearing gabbros (see below) does clinopyroxene assume any importance as a cumulus phase.

5.5 CUMULATE GABBROS*

5.5.1 Field Relations

Cumulate gabbros are restricted to the type area of PBOC (Fig. B-1) where they lie between amphibolitized olivine norites (locality 3) to the north and low-Ti dolerites to the south (Map 1). For the most part these rocks are intensely sheared and pervasively weathered and contacts with adjacent lithologies are not exposed. Shearing, however, is most intense in the vicinity of these contacts, and boundaries are almost certainly faulted. Essentially undeformed blocks of cumulate gabbro ranging in size from several tens of centimetres to several tens of metres are scattered throughout the highly sheared matrix. A thin (15-35 cm wide), amphibolitized low-Ti basaltic dyke cuts one of the larger gabbro outcrops at GR 6438, 8132 , thus implying at least a spatial link between these gabbros and the overlying low-Ti basalts (Fig. 5.1).

---

* In the classification of Streckeisen (1976) these rocks are more strictly termed quartz-bearing gabbronorites.

5.5.2 Petrography

In approximate order of decreasing abundance, primary phases in these PBOC gabbros include plagioclase, clinopyroxene, orthopyroxene, quartz, and a trace of Fe-Ti oxide. Approximate modes fall in the ranges (%): opx 10-25, plag 40-50, cpx 20-30, qz 2-10.

Plagioclase is remarkably fresh but clinopyroxene is variably uralitized and orthopyroxene is often partially or, on occasion, wholly replaced by serpentine minerals ± talc and/or uralite assemblages. As in the olivine norites, intense amphibolitization in these gabbros is confined to shears and microshears. However, pyroxenes only several millimetres away from microshears may be practically unaltered (e.g. 026) and plagioclase is fresh throughout.

The cumulate gabbros are medium-grained (most grains fall in the range 0.5mm-3mm) and display textures transitional between adcumulus and intergranular types. Orthopyroxene and plagioclase grains are typically euhedral with minimal development of irregular outgrowths. Outgrowths on clinopyroxene grains are often relatively well-developed, but only to the extent that they might poikilitically enclose one or two plagioclase grains. Quartz invariably displays an interstitial habit. Fe-Ti oxide is intergranular in the more Fe-poor gabbros (e.g. 025-027, see Table 5.4) but may also form inclusions in clinopyroxene in the relatively Fe-rich gabbros (e.g. 029). Secondary amphibole is most abundant in the Fe-rich gabbros where it may replace up to 50% of the total pyroxene.

5.5.3 Mineral Chemistry

In these PBOC gabbros:

(i) Most orthopyroxenes are bronzites ($70 < mg < 79$) which display slight normal zoning (Table C-9). In the more Fe-rich gabbros (e.g. 028) bronzites coexist with relatively Mg-rich hypersthene ($mg > 60$; Fig 5.5). Minor element abundances in these orthopyroxenes fall in the following ranges: $TiO_2 < 0.07\%$; Al_2O_3, 0.8%-1.6%; $Cr_2O_3 < 0.4\%$; MnO, 0.15%-0.4%; CaO, 2%-2.5%; and, $Na_2O < 0.1\%$.

(ii) Clinopyroxenes are predominantly Ti- and Na-poor augites, although some Fe-rich diopsides do occur ($Ca_{48}Mg_{43}Fe'_9$ to $Ca_{44}Mg_{36}Fe'_{20}$;

e.g. Table C-9). The Ca-rich pyroxenes are not significantly zoned but in the relatively Fe-rich gabbros (e.g. 028) they display considerable grain-to-grain variation in *mg* value and Cr_2O_3 content (*mg* 80-65, Cr_2O_3 < 0.6%; Table C-9, Fig. 5.5). Those in the more Fe-rich gabbros also tend to be more Ca-rich than their counterparts in the relatively Mg-rich variants (Fig. 5.5). On average, Ca-rich pyroxenes in these gabbros are enriched in Al_2O_3 (1.5%-3.0%), Al^{VI} (Fig. 5.7) and Cr_2O_3 (<0.75%) relative to coexisting Ca-poor pyroxenes, and the former display trends of rapidly decreasing Al_2O_3 and Cr_2O_3 with decreasing *mg*.

(iii) Plagioclase is K-poor (<0.06% K_2O) bytownite displaying a relatively restricted range in composition (An_{88-81}; e.g. Table C-5, analyses 1,2). Most grains are chemically homogeneous although some display slight normal or reverse zoning. Compared to bytownites in the PBOC olivine norites these are significantly enriched in Fe (0.6%-0.9% ΣFeO) and slightly enriched in Mg (∿0.1% MgO, e.g. Table C-5). On average, these bytownites appear to be slightly enriched in Fe relative to plagioclases in somewhat similar MORG (generally <0.7% ΣFeO, e.g. Hodges and Papike, 1976), although few data on the latter are available.

(iv) Reconnaissance microprobe analyses (not listed) suggest that the Fe-Ti oxides are largely, if not entirely, ilmenite.

(v) Secondary amphiboles are relatively Al-rich, Na-poor actinolites (Fig. 5.8; Table C-6, analyses 9,10). Compared to secondary amphiboles in PBOC olivine-bearing intrusives they are significantly enriched in Fe (ΣFeO = 12%-16%, M = 75-65, e.g. Table C-6), MnO (0.2%-0.4%) and TiO_2 (0.1%-0.3%). In fact, their TiO_2 contents appear to be anomalously high considering the low TiO_2 in their pyroxene precursors (<0.07%, Table C-9) and the low bulk TiO_2 (<0.2%) in these gabbros. Overall, these actinolites display a more restricted range in chemistry than secondary amphiboles in MORG (*cf.* Helmstaedt and Allen, 1976; Hodges and Papike, 1976; Prichard and Cann, 1982) and in mafic intrustives in ophiolites (e.g. Mevel *et al.*, 1978; Liou and Ernst, 1979; Stern and Elthon, 1979).

In the PBOC gabbros, actinolites replacing undeformed pyroxenes are chemically similar to coexisting actinolites occurring in distinct

microshears. In common with the magnesiohornblendes in the PBOC olivine norites, actinolites in the gabbros are relatively Cl-poor (<0.1% Cl). This might suggest that seawater (19 wt% Cl; Mason, 1966) was not the fluid phase involved in the formation of these amphiboles. However, in hydrothermally altered MORG from Gettysberg Bank (northeastern Atlantic), Prichard and Cann (1982) found that actinolites coexisting with relatively Cl-rich secondary hornblendes (containing up to 0.4% Cl) are invariably Cl-poor (<0.05% Cl). Consequently it would appear that under at least some seafloor hydrothermal conditions, actinolite which crystallized in the presence of seawater need not be necessarily enriched in Cl. Thus, the data available do not exclude the possibility that uralitization of the PBOC gabbros may reflect some hydrothermal interaction with seawater.

5.5.4 Whole-Rock Chemistry

Although the *mg* values of the more Mg-rich PBOC gabbros (*mg* ∿ 77) are only slightly lower than those of the more evolved PBOC olivine norites (*mg* ∿ 81), the gabbros are significantly enriched in *di* and normative plagioclase (*ab* + *an*) relative to the latter (compare Tables 5.3 and 5.4b, see Fig. 5.2). Some of the more plagioclase-rich olivine norite variants (e.g. Table 5.3, analysis 6) have normative plagioclase and normative clinopyroxene contents (Fig. 5.2) comparable to the gabbros, but these norites have significantly higher *mg* values (89-85), and higher normative olivine at the expense of normative orthopyroxene (Fig. 5.2). However, following significant saussuritization, these particular olivine norite variants display, among other changes in their chemistries, varying degrees of secondary depletion in Si and depletion or enrichment in Ca (see Appendix A). Consequently, their pristine CATION normative CPX, OPX and OL almost certainly have been modified significantly (e.g. samples 328 and 329 contain insufficient SiO_2 to form the required normative minerals; Table B-7, analyses 9,10) and apparent normative similarities to the gabbros may be largely fortuitous.

In addition to being enriched in Al and Ca relative to the evolved olivine norites, the gabbros are also slightly enriched in most large-ion lithophile (LIL) elements (e.g. Rb, Ba, Sr) and incompatible elements (e.g. Ti, P, Zr, Y). In fact, the gabbros themselves display general trends of increasing LIL, alkali, chalcophile and incompatible element abundances with decreasing *mg* (Table 5.4). However, despite these relative enrichments the PBOC gabbros remain somewhat depleted in

TABLE 5.4a

Major and Trace Element Analyses of Gabbros from the Pigna Barney Ophiolitic Complex

ANALYSIS No.	1	2	3	4	5
SAMPLE	025	026	027	028	029
SiO_2	50.96	51.37	51.24	51.46	51.72
TiO_2	0.08	0.07	0.08	0.14	0.17
Al_2O_3	16.08	14.75	15.72	16.21	15.37
Cr_2O_3	0.17	0.20	0.16	0.07	0.04
Fe_2O_3	0.42	0.46	0.44	0.55	0.61
FeO	6.00	6.58	6.35	7.87	8.74
NiO	0.03	0.03	0.03	0.01	0.01
MnO	0.15	0.15	0.15	0.17	0.17
MgO	12.33	13.35	12.54	9.16	8.48
CaO	12.83	12.18	13.12	12.92	12.51
Na_2O	0.96	0.84	1.05	1.29	1.29
K_2O	0.02	0.02	0.03	0.03	0.04
P_2O_5	0.04	0.03	0.04	0.04	0.05
TOTAL	100.07	100.03	100.95	99.92	99.20
ΣVol^1	1.45	1.29	1.72	2.13	2.41
FeO^1	5.56	6.22	5.89	7.14	7.60
mg	77.1	76.9	76.4	65.7	61.5
TRACE ELEMENTS (ug/g)					
K	177	160	250	288	311
Rb	1	1	1	1	1
Ba	5	5	7	6	11
Sr	15	10	17	6	19
Li	2.2	10.0	2.9	2.3	2.3
Zr	3	4	3	6	9
Y	7	4	6	11	13
Nb	3	3	3	3	3
Ti	565	541	560	902	1074
Cu	33	35	37	70	82
Zn	49	56	54	65	70
Ni	206	228	212	109	111
Co	56	68	84	73	65
V	148	147	152	228	255
Cr	1189	1301	1112	471	288
Sc	45	n.d.	n.d.	55	n.d.

mg = 100 Mg/(Mg+ΣFe+MN)

[1] See Appendix G (Fe_2O_3/FeO adjusted to 0.07)

n.d. = not determined.

Major element analyses are recalculated to original totals on a volatile-free basis. Trace element values are also recalculated on a volatile-free basis.

TABLE 5.4b

C.I.P.W. Normative Mineralogy of Gabbros from the Pigna Barney Ophiolitic Complex

ANALYSIS No.	1	2	3	4	5
SAMPLE	025	026	027	028	029
qz	-	0.29	-	1.73	3.23
or	0.12	0.12	0.18	0.18	0.24
ab	8.12	7.11	8.88	10.92	10.92
an	39.51	36.42	38.09	38.35	36.03
di	19.16	19.10	21.47	20.75	21.05
hy	31.60	35.83	28.47	26.73	26.36
ol	0.46	-	2.75	-	-
mt	0.61	0.67	0.64	0.80	0.88
chr	0.25	0.29	0.24	0.10	0.06
il	0.15	0.13	0.15	0.27	0.32
ap	0.09	0.07	0.09	0.09	0.12
Σ	100.07	100.03	100.96	99.92	99.21
100 *an*/(*ab*+*an*)	83.0	83.7	81.1	77.8	76.7

Fe_2O_3/FeO adjusted to 0.07 (see Appendix G).

these elements compared to the majority of MORG and ophiolitic gabbroic intrusives with similar MgO contents (*cf.* Section 5.4.4, e.g. Fig. 5.10). They display a relatively restricted Fe-enrichment trend intermediate between that of the PBOC olivine norites and that of MORG (Fig. 5.10). Some Troodos and Vourinos gabbros display similar $\sum FeO:\sum FeO/MgO$ relations, although the overall ranges of $\sum FeO:\sum FeO/MgO$ variation in gabbros from these ophiolites are considerably more extensive (Fig. 5.10).

Discussion

Most aspects of the chemistry of these PBOC gabbros suggest that they crystallized from liquids similar to, but slightly more evolved (i.e. slightly enriched in *di*, *qz*, *ab*, Fe/Mg, and incompatible elements) than, those from which the associated olivine norites were derived. Coexisting olivines and orthopyroxenes in the PBOC olivine-bearing cumulates display a regular variation in Fe:Mg relations where $M(opx) = 0.9\ M(ol) + 9$ ($r^2 = 0.97$, Table C-2, *cf.* Fig. D-2). Assuming $D^{ol\text{-}liq}_{Fe\text{-}Mg} = 0.3$ (e.g. Roeder and Emslie, 1970) for these intrusives, and assuming that $D^{opx\text{-}liq}_{Fe\text{-}Mg}$ for melts in equilibrium with olivine + orthopyroxene is similar to that for saturated or slightly *qz* normative melts crystallizing orthopyroxene (± quartz) in the absence of olivine, then, on the basis of their orthopyroxene compositions (e.g. Table C-9), the PBOC gabbros appear to have crystallized from melts whose *M* values ranged from *ca.* 51 to 31. For $D^{cpx\text{-}liq}_{Ti} \sim 0.3$ (Pearce and Norry, 1979) these parental liquids appear to have been Ti-poor (<0.3% TiO_2) and the crystallization of relatively late-stage ilmenite rather than titanomagnetite from such melts strongly suggests that fO_2 and presumably P_{H_2O} were particularly low, especially for melts with *M* values as low as those inferred from *M* opx. Furthermore, the relatively small charge excesses and, on occasion, charge deficiencies in the pyroxenes (e.g. Table C-9) suggest that these phases are depleted in Fe^{3+} (see page 84) and reinforce the conclusion that their parental magmas were strongly reduced. Although the measured Fe_2O_3/FeO ratios in the more Mg-rich gabbros remain relatively low ($Fe_2O_3/FeO \sim 1$), presumably these have been significantly increased by secondary alteration (see Section 5.5.2). Consequently, the Fe_2O_3/FeO ratios in the analyses listed in Table 5.4 have been adjusted to that of the most evolved (and freshest) PBOC olivine norite (sample 440, $Fe_2O_3/FeO = 0.07$).

In addition to being Ti-poor, the melts from which these gabbros crystallized appear to have been strongly depleted in other incompatible

elements (e.g. Zr and P, *cf.* Table 5.4a). One highly distinctive characteristic of the PBOC gabbros and olivine norites (and the low-Ti basalts, see Section 5.7.4) which, perhaps above all else, suggests that they are genetically related is the fact that their Zr/Y ratios are consistently ≤ 1. This chemical characteristic appears to be unique to the PBOC and nearby low-Ti basaltic rocks in the Woolomin beds and, ultimately, it most probably reflects unusually low Zr/Y ratios in the primary PBOC melts and/or in their mantle source area (see Sections 5.7.4 and 5.8).

5.6 LOW-Ti DOLERITIC INTRUSIVES

5.6.1 Field Relations

These are a somewhat enigmatic group of altered doleritic intrusives which form, and are apparently confined to, one or more relatively small fault blocks in the type area of the PBOC (Map 1, *cf.* Fig. B-1). By analogy with other ophiolitic complexes and ophiolites in general (e.g. Coleman, 1977) these PBOC intrusives probably represent a fragment of a once-continuous doleritic layer lying between the PBOC gabbros and basaltic extrusives.

On occasion, contacts between adjacent low-Ti doleritic intrusives are relatively well-exposed, although both the upper and lower contacts of any single cooling unit have not been observed. Consequently, the thicknesses of these units are not known with any accuracy, but they appear to range from approximately 5 metres to several tens of metres. Some intrusive contacts are slightly irregular on a mesoscopic scale but, on present exposures and field orientations (perhaps influenced by faulting), the overall form-surfaces of these intrusives suggest that they constitute a more-or-less monolithological sequence of sills and/or low-angle dykes which dip moderately (40°-70°) to the south and southwest. Because these PBOC intrusives were emplaced within a sequence which appears to entirely consist of similar sill-like doleritic intrusives, they may constitute part of what might be termed a sheeted sill complex. Unlike sheeted dyke sequences in some ophiolites (e.g. Troodos and Bay of Islands), these sills do not appear to display the one-way chilling characteristics indicative of repetitive magma injection along a single axis of intrusion (e.g. Kidd and Cann, 1974; Kidd,1977). This suggests that: (i) they are not a sheeted dyke sequence which has been rotated

during disruption of the PBOC, and (ii) they were probably successively emplaced as discrete cooling units underlying the extrusive carapace of the PBOC.

5.6.2 Petrography and Mineral Chemistry

These PBOC intrusives are highly altered quartz-bearing "dolerites" which typically display fine-to medium-grained relict intergranular textures. The chemistries of the principal primary and secondary phases are known for only one of these intrusives (032).

Originally, these doleritic intrusives consisted of: (i) clinopyroxenes which, in sample 032 at least, are slightly zoned, relatively calcic augites (Fig. 5.5) strongly depleted in Ti, Cr and Na (e.g. Table C-9, analyses 11, 12); (ii) plagioclase, on occasion at least as calcic as sodic labradorite (sample 030, optical determinations); (iii) Fe-Ti oxides which appear to have been largely titanomagnetite, but possibly accompanied by rare (?) chromite in sample 030; (iv) intergranular quartz, often forming graphic intergrowths with plagioclase (now albitized); and possibly, (v) minor (?) primary prismatic, pleochroic brown-green amphibole (? hornblende) in sample 031. Modal abundances of primary intergranular quartz range from approximately 1% in sample 030 to approximately 30% in sample 033. Secondary quartz appears to be confined to carbonate ± quartz veins which are relatively abundant in most outcrops (but absent from the samples analysed, see below). Fe-Ti oxides typically constitute less than *ca.* 2% of the mode.

Typically, clinopyroxene is almost entirely uralitized (actinolitic hornblende in sample 032, Table C-6, analysis 11) and/or partially replaced by epidote ± chlorite. Plagioclase is usually albitized, almost invariably kaolinized (often highly so, e.g. 034) and, on occasion, partially or wholly replaced by prehnite ± chlorite ± sericite. Fe-Ti oxides are almost invariably hydrated (transluscent, cloudy, dull-brown, microprobe analysis totals as low as 70%) and, on occasion, altered to (?) leucoxene and/or rare sphere (e.g. 034, 035). Primary quartz displays strain extinction.

5.6.3 Whole-Rock Chemistry

Because these rocks are pervasively altered their bulk chemistries must be interpreted with considerable caution. For example, modal quartz significantly exceeds normative *qz* in all samples. At least in part,

this might result from the albitization of plagioclase and some loss of Ca relative to Fe and Mg, thus increasing *ab* and *hy* at the expense of *qz*. Intense kaolinization of albite also appears to have resulted in some loss of Na, especially in sample 031 (Table 5.5a, analysis 2).

Although sample 030 appears to have close chemical affinities with the more Fe-rich PBOC low-Ti basaltic extrusives (e.g. Fig. 6.1; compare analysis 1, Table 5.5a, with analyses 11-13, Table 5.6a), by comparison the remainder of the low-Ti doleritic intrusives are significantly enriched in SiO_2 (Fig. 5.15), incompatible elements (e.g. Ti, P, Zr) and, to a lesser extent, LREE. The latter intrusives also have relatively high $Al_2O_3/(Al_2O_3 + \Sigma FeO + MgO)$ and Al/(Al + Fe + Ti + Mg) ratios, and low Mg/(Mg + Si + Al) ratios (Figs 5.13C,D; 6.1c) suggesting affinities with the island arc tholeiitic or calc-alkaline series, although it must be emphasized that pristine Fe and/or Mg abundances (at least) might have been modified somewhat during secondary alteration. Nevertheless, their relatively low Ti, Zr, Ni, Cr and Y abundances (Figs 5.16, 5.17, 6.1f,h,i,j), low Ti/V and $\Sigma FeO:\Sigma FeO/MgO$ ratios (Fig. 5.10, *cf.* Fig. 3.19), high Sr relative to Ti and Zr (Fig. 6.1b), and the presence of significant modal quartz (? + rare primary amphibole, see Section 5.6.2), are all consistent with a comparison to Si-rich IAT, or perhaps incompatible-element-depleted CAB. Miyashiro (1973b, 1975, 1975b,c, 1977) argued that somewhat similar Si-rich, Mg-poor basaltic rocks in several ophiolites [e.g. Troodos (see Fig. 5.10), Vourinos, Pindos and perhaps including a number of North American examples (*cf.* Upadhyay and Neale, 1979)] have calc-alkaline affinities*. On this basis Miyashiro (*op.cit.*) concluded that the host ophiolites were generated in oceanic island arc settings. However, in common with the PBOC examples, these rocks typically display considerable relatively low-grade metamorphic and/or hydrothermal mineralogical and possibly chemical reconstitution, and for this reason Miyashiro's (*op.cit.*) conclusions have been disputed (see Smith, 1975 for a summary; Church and Coish, 1976). Similarly, it is unclear whether the PBOC low-Ti doleritic intrusives might be calc-alkaline or tholeiitic (probably the latter, despite only limited Fe-enrichment; see below), and in this context, their implications for the remainder of the PBOC ophiolitic lithologies are somewhat enigmatic.

Discussion

Although sheeted dyke sequences are perhaps more characteristic of the majority of ophiolites (e.g. Coleman, 1977; Kidd, 1977), sheeted

* Recent microprobe analyses of optically fresh glasses in Troodos pillows (Robinson *et al.*, 1981) reinforce Miyashiro's arguments. These glasses range in composition from basalt-rhyodacite and have calc-alkaline affinities.

TABLE 5.5a

Major and Trace Element Analyses of Doleritic Intrusives from the Pigna Barney Ophiolitic Complex

ANALYSIS No.	1	2	3	4	5
SAMPLE	030	031	032	033	034
SiO_2	53.93	57.55	55.30	56.61	57.17
TiO_2	0.24	0.51	0.54	0.52	0.37
Al_2O_3	13.50	15.48	15.62	15.74	15.10
Fe_2O_3	2.41	1.91	2.79	3.22	2.81
FeO	9.05	7.04	6.74	5.77	7.40
MnO	0.22	0.15	0.17	0.16	0.17
MgO	8.01	5.63	5.49	4.90	4.68
CaO	7.87	8.67	8.96	9.44	8.01
Na_2O	4.34	1.77	3.04	2.56	3.96
K_2O	0.11	0.56	0.55	0.05	0.13
P_2O_5	0.03	0.13	0.10	0.14	0.06
TOTAL	99.71	99.40	99.30	99.11	99.86
ΣVol[1]	3.02	3.40	3.59	3.84	3.38
$\Sigma FeO/MgO$	1.40	1.56	1.69	1.77	2.12
		TRACE ELEMENTS (µg/g)			
Rb	<2		8	2	<2
Ba	24		n.d.	17	44
Sr	92		161	180	112
Li	4.0		2.9	3.4	5.2
Zr	10		n.d.	39	19
Nb	3		n.d.	<3	<3
Y	18		13	18	12
Ti[1]	1617		n.d.	3126	2307
Cu	123		139	144	49
Zn	101		102	94	88
Ni	97		17	50	17
Co	<65		36	45	65
V	345		n.d.	319	290
Cr	204		n.d.	84	38
La	5		5	10	7
Ce	6		19	17	11
Nd	-		7	9	5

[1] See Appendix G. n.d. = not determined.

Major element analyses are recalculated to original totals on a volatile-free basis. Trace element values are also recalculated on a volatile-free basis.

TABLE 5.5b

C.I.P.W. Normative Mineralogy of Doleritic Intrusives from the Pigna Barney Ophiolitic Complex

ANALYSIS No.	1	2	3	4	5
SAMPLE	030	031	032	033	034
qz	-	14.59	5.64	12.64	6.26
or	0.65	3.31	3.25	0.30	0.77
ab	36.81	14.98	25.81	21.75	33.59
an	17.04	32.67	27.39	31.37	23.08
di	18.01	7.87	13.66	12.14	13.62
hy	14.52	23.26	20.80	19.21	20.08
ol	10.35	-	-	-	-
mt	1.81	1.45	1.49	1.41	1.61
chr	0.04	-	-	0.01	0.01
il	0.46	0.97	1.03	0.99	0.70
ap	0.07	0.30	0.23	0.32	0.14
Σ	99.76	99.40	99.30	100.14	99.86
100 an/(ab+an)	31.6	68.6	51.5	59.1	40.7

$Fe^{3+}/\Sigma Fe = 0.1$

sill complexes are well-developed in the Coast Range Ophiolite of California (e.g. Hopson and Frano, 1977), and in ophiolite from the Ergani district, Turkey (Bamba, 1974). In assigning an oceanic spreading centre mode of origin to the Point Sal Ophiolite, Hopson and Frano (1977) interpreted the doleritic sheeted-sill complex occurring between the volcanic and plutonic parts of this ophiolite to represent second-stage*, relatively more primitive melts emplaced during the initiation of a new spreading centre within pre-existing oceanic crust. The PBOC has few petrological characteristics in common with ophiolites inferred to have been generated in mid-ocean ridge settings, and it is considered unlikely that the low-Ti doleritic intrusives were emplaced in the manner proposed for the Point Sal sheeted sill complex. Furthermore, unlike the Point Sal sills, these PBOC intrusives are significantly more evolved, both chemically and mineralogically, than the associated extrusives and intrusives. This might suggest that they were emplaced during the waning stages of igneous activity in the PBOC.

On the basis of its chemistry, at least one PBOC low-Ti dolerite (030) simply appears to be a slightly Fe-rich intrusive equivalent of the overlying low-Ti basalts (see Figs 5.13, 5.15, 6.1). Although enriched in Si and the relatively immobile incompatible elements (e.g. Ti, P, Zr), the remaining doleritic intrusives are significantly depleted in Fe relative to compositions which might be expected to be direct fractionates of melts similar in composition to the PBOC low-Ti basalts (e.g. Figs 5.10, 5.13D).

Although the doleritic intrusives might have lost some Fe during alteration, it is unlikely that this could account for all of the Fe-depletion in these rocks relative to the extrusives because: (i) most pyroxenes in the low-Ti doleritic rocks are entirely replaced by amphiboles which are relatively Fe-rich (e.g. Table C-6, analysis 11), or apparently relatively Fe-rich (deep green colouration); (ii) in the intrusives, modal amounts of Fe-Ti oxide are relatively minor (<2%) and these appear to retain much of their original Fe (at least 60%-70%, reconnaissance microprobe analyses). It is also unlikely that this Fe-

---

* Not to be confused with the postulated *en*-rich second-stage MORB of Duncan and Green (1980). However, Hopson and Frano (1977) do record the presence of very late-stage bronzite-rich microgabbro dykes in the Point Sal plutonic sequence. Perhaps these warrant further investigation in terms of the Duncan and Green (1980a,b) model.

depletion is the result of fractionation of Fe-Ti oxides from melts similar in composition to the low-Ti basalts because: (i) the latter appear to have been unusually impoverished in Fe^{3+} (see Sections 5.7.3 and 5.7.4), and the observed two-fold enrichment in TiO_2 in the doleritic intrusives relative to the extrusives is inconsistent with signficiant fractionation of Fe-Ti oxides at low fO_2, and (ii) the predominantly intergranular habits of the Fe-Ti oxides in the doleritic intrusives suggest that they appeared at a relatively late stage in the crystallization history of these rocks.

In general terms, however, the low incompatible element contents of these doleritic intrusives relative to basaltic rocks in the Glen Ward beds (see Chapter 3) suggest that the former have close affinities with the PBOC. In this context, the uncharacteristically high Zr/Y ratios in two of the low-Ti doleritic intrusives (Zr/Y = 1.6, and 2.2, Table 5.5a; Zr/Y $\leq$ 1 for other PBOC lithologies, e.g. Fig. 5.16, Tables 5.4a and 5.6a) suggest that Zr abundances in the melts from which they crystallized may have been several times greater than those in other PBOC melts. Alternatively, the relatively high Zr/Y ratios inthe doleritic intrusives might suggest that they crystallized from evolved "PBOC melts" (i.e. initially having low Zr/Y) which had experienced fractionation of significant quantities of: (i) phases such as olivine ± plagioclase ± orthopyroxene which are relatively impoverished in Zr and, to a lesser extent, Y (*cf.* Pearce and Norry, 1979), thus significantly increasing Zr + Y, and slightly increasing Zr/Y in the residual melt; and (ii) phases possessing significant quantities of Y and low Zr/Y ratios, of which clinopyroxene is perhaps the only likely candidate ($D_{Zr}^{cpx-liq}$ = 0.1, $D_{Y}^{cpx-liq}$ = 0.5, Pearce and Norry, 1979). Because Zr and Y abundances in the relatively unfractionated parent melts are likely to have been low (? < 1 µg/g), fractionation models based on these elements are subject to very large uncertainties. In particular, these include non-ideal partitioning at low concentrations, and large variations in the Zr/Y ratio for small variations in Zr and/or Y. However, to a first approximation it would appear that it might be necessary to remove at least 50-60 vol. % of clinopyroxene from a melt of low-Ti basalt composition (e.g. Zr $\sim$ 10 µg/g, Y $\sim$ 15 µg/g, *cf.* Table 5.6a) to generate a liquid with a Zr/Y ratio significantly greater than one. Such high degrees of fractionation lead to more significant Fe-enrichment in the doleritic rocks and depletion in Ni and Cr relative to that observed in 033 (Ni = 50 µg/g, Cr = 84 µg/g; Table 5.5a). To satisfy the constraints imposed by Fe, Ni and Cr abundances in the low-Ti doleritic intrusives, it would seem that

their parent melts initially may have had higher Zr/Yratios (and perhaps higher Si) than other envisaged PBOC melts, or they gave rise to a range of cpx- and Fe-rich cumulates not preserved in the PBOC.

5.7 BASALTIC EXTRUSIVES AND FINE-GRAINED BASALTIC INTRUSIVES

These members of the PBOC are found only in the vicinity of the type area and are best exposed in Tomalla Creek between GR6379,8100 and GR6305,8038. Also, several small blocks (<20 sq m outcrop) occur within serpentinite along the north bank of the Pigna Barney River between GR640,818 and GR6464,8181. Overall, they differ from basaltic rocks in the Myra beds and Glen Ward beds in their general field characteristics (Section 5.7.1) and in their textures, mineralogy and chemistry (Sections 5.7.2 to 5.7.4, respectively). On the basis of their most distinctive chemical characteristics these PBOC basaltic rocks are termed low-Ti basalts (*cf.* Sun and Nesbitt, 1978). Low-Ti basalts have not been found in the Tamworth Belt succession. However, altered basaltic rocks having some characteristics in common with the PBOC low-Ti basalts have been reported recently from the Woolomin beds in the Glenrock Station area (Offler, 1982).

5.7.1 Field Relations

Within and near the type area of the PBOC low-Ti basaltic rocks crop out intermittently over an area of approximately 2.5 sq km (Map 1). Some outcrops of basaltic rocks similar to those in the Glen Ward beds (see Chapter 3) also occur in this area. Contacts between these and the low-Ti basaltic rocks are not exposed. In some outcrops the Glen Ward types in this area are pervasively sheared (e.g. GR630,820) or have sheared margins. Shear zones are also common within the low-Ti basalt outcrops and it is likely that the two basalt types have been tectonically mixed. However, most of these Glen Ward types are fine to medium-grained dolerites, and from the evidence available, the possibility that at least some might have intruded the low-Ti basalts cannot be completely discounted.

In outcrop, fresh low-Ti basaltic rocks are pale purplish-grey in colour while the more altered examples are pale grey-green to olive green. Myra and Glen Ward basaltic rocks are almost invariably deep green to greenish-black or brownish black. The two types are usually distinguishable solely on the basis of colour alone but in many parts of this area shearing and/or weathering have modified or obliterated these and other distinctive field and petrographic characteristics.